

MEASUREMENT OF ENERGY SPECTRUM OF ELECTRONS FIELD-EMITTED FROM
DIAMOND FIELD-EMITTER ARRAYS

By

Christopher L. Stewart

Senior Honors Thesis

Submitted to the Faculty of the

Department of Physics and Astronomy of Vanderbilt University

in partial fulfilment of the requirements for

DEPARTMENTAL HONORS

in

Physics

May, 2009

Nashville, Tennessee

Advisor: Charles A. Brau

Honors Thesis Committee:

Jim L. Davidson

Norman H. Tolk

David A. Weintraub

Abstract

A retarding mesh analyzer was used to measure the electron energy spectrum field emitted from a single tip of a Diamond Field Emitter Array. The emission was dominated by adsorbed gas atoms and molecules on the surface which were both spatially and temporally unstable. As a result, the spectra taken had highly variant spectral features and there was an order of magnitude span in the emitted current. The spectrum from a clean surface roughly obeyed the thermal field emission model and was consistent with reported spectra from a nitrogen-doped, diamond-like carbon film.

I. Introduction

Electron-beam sources find application in widely used instruments, especially in high-resolution microscopes and in free-electron lasers. Conventional electron microscopy techniques have resolutions which are dependent on the brightness of the imaging beam; although great strides have been made which have allowed for the production of ever-brighter electron beams, there is a quantum limit placed on the brightness of a beam. The production of beams with brightness approaching the quantum limit which could be used in conventional electron microscopes would greatly increase the usefulness of such devices. In addition to improvements upon existing designs, new imaging techniques could be developed which take advantage of quantum properties of high-brightness beams. One such method is an anti-coincidence measurement which relies on Pauli exclusion to induce arrival time statistics more uniform than could be expected by a Poissonian distribution. The method was originally conceived by Hanbury Brown and Twiss as a means to resolve distant stars using boson bunching; fermion anti-bunching would essentially be the opposite effect. A very weak anti-bunching effect was measured recently in a beam with a degeneracy of about 10^{-4} [6]; making the same measurement on a beam with order-of-unity degeneracy would be simpler. The ability to use such beam properties requires a beam near the quantum limit of brightness, which makes reliable, very-high-brightness sources uniquely suited to such a technique. Such sources are also ideal as cathodes in free electron lasers of tabletop or smaller dimensions,

since they emit a large amount of current into a small transverse area.

Brightness as a quantitative aspect of electron beams arises from their properties as viewed in phase space. 6-dimensional phase space is divisible into discrete cells of volume h^3 ; these cells can each hold at most 2 electrons due to the antisymmetry requirements of Pauli exclusion. The degeneracy of a beam of electrons is the ratio of the 6D density of electrons to the theoretical maximum:

$$\delta = \frac{h^3 d^6 N_e}{2 dx dp_x dy dp_y dz dp_z}$$

where N_e is the number of electrons; x , y , and z are the position coordinates; and p_x , p_y , and p_z are the momenta in each respective direction.

The transverse brightness is the current per unit area per unit solid angle; it is often normalized to remove the dependence on beam energy; the normalized brightness is

$$B_N = \frac{B}{\beta^2 \gamma^2} = \frac{2m^2 c^2 q \Delta E}{h^3} \delta$$

For many applications, particularly those which use interaction with some medium to extract energy from the beam, the transverse properties define the extent of the interaction region in phase space, so the 4-D phase space image of the beam is indicative of beam quality.

The majority of cathodes currently used to produce electron beams for the above applications currently fall into three categories: photocathodes, thermionic cathodes, and field emitters. Photocathodes take advantage of the photoelectric effect by striking a surface with a laser pulse to liberate electrons; they produce high currents, but are vulnerable to laser damage during use and to contamination by residual gases in the vacuum system. Thermionic cathodes are heated to high temperatures ($>1000\text{K}$) such that the energy distribution of the electrons within the cathode has a high-energy tail which surmounts the potential barrier. Thermionic cathodes behave very predictably with respect to operating temperature and current production, and in addition are robust against atmospheric contamination. They have a very small energy spread (on the order of 0.1eV), lending them to applications in which a monochromatic beam is ideal. However, the nature of their

use means that they endure very high thermal stresses from being cycled between hot and cold, and they have a very high emittance, which requires intricate beam focusing before the beam can be put to use. Field emitters use an applied external field on sharp geometric surfaces to induce high tunneling rates from the cathode, and depending on the cathode material, can be resistant to both contamination and to degradation resulting from use. Field emitters tend to produce lower currents than the other two types of cathode; this can be remedied by applying a field to an array of sharp tips. The methods of electron emission are shown in Figure 1.

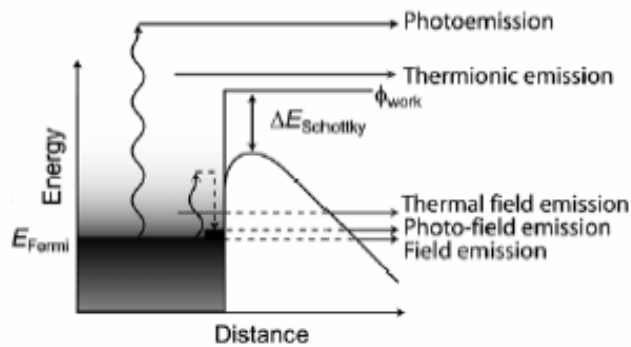


Figure 1: Methods of freeing electrons from cathodes. [7]

The Diamond Field Emitter Array (DFEA) used in this experiment was produced at Vanderbilt University via chemical vapor deposition. The physical structure of each emitter in the array is that of a square-base pyramid which has at its peak 1 or 2 needle-like tips with tip radius on the order of ~5-10nm. The dimensions of the tip are somewhat similar to a multi-walled carbon nanotube, but with a smaller aspect ratio. The diamond is doped with boron and nitrogen and the tip composition is expected to be of the same content, though this is unconfirmed and joule heating of the tips during emission may heat them significantly enough to change the condition of the surface.

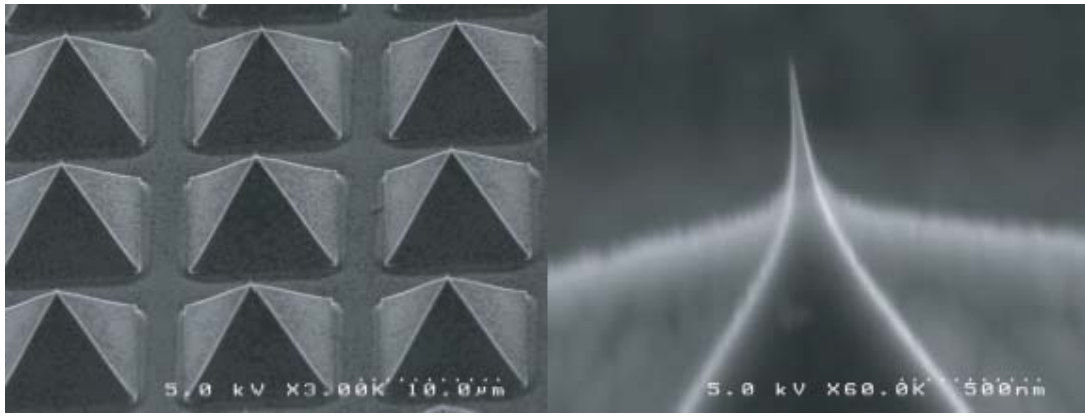


Figure 2: SEM images of a DFEA similar to the one used in the experiment. Left: arrangement of pyramidal bases. Right: close-up view of a single tip. [8]

The measurement of the energy spectrum of the emitted electrons from a DFEA is important for multiple reasons. First, it gives an indication of the usefulness of the cathode in specific devices which may have constraints on how wide the electron energy spread can be – for example in imaging. Second, the measurement provides physical information about the bare surface of the diamond emitter and, due to the presence of adsorbates, about their surface interactions during field emission and whether or not they can be used in a predictable manner toward a specific end. We expect to see an energy spectrum which is approximately predicted by the Fowler-Nordheim theory for field emission from metals, with slight deviation on the low-energy tail of the distribution.

II. Theory

The discussion of the development of Fowler-Nordheim theory follows [1]. In 1928, Fowler and Nordheim used the newly demonstrated phenomenon of quantum tunneling to describe the emission of electrons from a metal cathode under a strong applied electric field. The applied field lowers the potential outside the cathode surface below the Fermi level of the cathode, providing a place into which the electrons can tunnel as real particles. The field also depresses the height of the potential barrier at the cathode surface due to the attraction of the electron to its image charge; this is known as the Schottky Effect, and can be seen in Figure 1. Once the electrons have tunneled outside the cathode, they are quickly accelerated away by the applied field, preventing tunneling

back into the cathode. The combination of these effects increases tunneling rates by several orders of magnitude, such that substantial current can be extracted. The electrons in the cathode are treated as a degenerate Fermi gas, and since the available cathodes at the time were metal, the electrons which had tunneled out of the cathode material were assumed to be replaced instantaneously.

The supply of electrons as a function of energy is derived from Fermi-Dirac statistics; it has the form [1]:

$$N(T, \varepsilon) = \ln\left(1 + e^{-\varepsilon/kT}\right)$$

where ε is the energy and k is the Boltzmann constant. In this experiment, some Joule-heating of the cathode during operation occurs, but the presence of a large heat sink and the low per-tip current levels keeps the energy tail on the supply function short – the cathode approximates a cold emitter. The transmission probability is a function of the work function ϕ (in eV), the applied field F in V/cm, and the electron energy ε (also in eV):

$$D(F, \varepsilon, \phi) = \exp\left[\frac{-6.83 \times 10^7 (\phi - \varepsilon)^{3/2} f(y)}{F}\right]$$

$f(y)$ is a dimensionless elliptic function of y used to account for the image charge effects, where

$$y = \frac{3.79 \times 10^{-4} F^{1/2}}{\phi - \varepsilon}$$

Multiplying the supply function and transmission probability and integrating over all electron energies gives the current density [1]:

$$J(\text{electrons} / \text{cm}^2 \cdot \text{sec}) = \int_{-\infty}^{\infty} cN(T, \varepsilon)D(F, \varepsilon, \phi)d\varepsilon$$

The theory predicts an energy spectrum which, unlike thermionic spectra, has a sweeping high energy feature which results from the tunneling effect. The theory also predicts a linear relationship between $1/V$ and $\ln(I/V^2)$. This relationship is a useful test to see how well a particular beam is characterized by Fowler-Nordheim theory. The theory, though developed for metals, has

shown remarkable success in predicting field emission properties of non-metals, most notably carbon nanotubes (CNTs).

DFEAs, which are similar to CNTs in chemical composition, show promise of also adhering to some degree to Fowler-Nordheim theory despite their classification as semiconductors. The fact that the resistivity of the material in bulk is several orders of magnitude higher than that of a metal alters the supply function for electrons in the cathode, making it dependent on the emission current and, therefore, the applied field. A deficit in electron supply may be mitigated by band-bending induced by the applied external field readily replenishing electrons. A second departure of the DFEA from metals results from the polycrystalline nature of the tips. The small grain size of the surface nanodiamond means that different crystal faces may be emitting from different tips, leading to slightly different work functions and different adsorbate binding properties between tips. This makes the ability of the analyzer to admit beamlet from only a single tip important in measuring the energy spread; if it cannot do so, artificial broadening of the spectrum may be introduced.

On top of the properties of the DFEA itself which may cause departure from Fowler-Nordheim predictions, the surface of the DFEA is inhabited by adsorbed molecules which are temporally unstable, both in position and in orientation to the tip; these result from the imperfect vacuum environment. The strength of the bond with the surface is dependent on the particular chemical species of adsorbate and its orientation with respect to the surface, which produces wide variance in the transience of adsorbates during any given operation time. The longevity of the bond with the surface is dependent on the temperature of the tip, since the probability of departure is proportional to a Boltzmann factor. A particular adsorbate will, during its lifetime on the DFEA, tend to migrate toward the tip, where the field is strongest. This preferential migration is due to the external field inducing a dipole moment in the adsorbate.

The presence of an adsorbed molecule will have three effects pertinent to field emission. First, since electric field enhancement occurs at sharp tips, the reduction of the tip radius from a few nanometers to a few or even one atomic width will boost the applied field at that point significantly.

Second, the work function of the surface is changed from that of the clean diamond tip to that of the adsorbed species in its particular orientation. Third, the presence of a potential well positioned outside the DFEA surface allows for electrons of certain energies to experience resonance effects [5] in their tunneling through the barrier. The energy at which this resonance occurs is a function of the spacing of the well from the original surface barrier and the depth of the well.

III. Experiment

The experimental apparatus used in the measurement of the energy spectrum of the DFEA allows for UHV operation, applied fields of up to 25MV/m before arcing, and in-situ adjustment of the tilt of the cathode plane with respect to the analyzer. The ambient pressure in the chamber was in the mid 10^{-10} Torr range, and while operating, rose to about 1.0×10^{-9} Torr. The anode bias was at ~ 2 kV. The DFEA under inspection was a 20×20 square array of $5 \mu\text{m}$ tips at a $100 \mu\text{m}$ pitch. This array size allowed for naked-eye alignment of the array with the aperture of the energy analyzer while ensuring that with typical cathode/anode spacing of a few hundred microns we would still be viewing only a single beamlet through the aperture.

The array was conditioned to approximately uniform emission across all emitting tips by thermally-assisted field evaporation techniques developed by Dr. Jarvis at Vanderbilt University [8]. Performing the uniformity conditioning prior to the measurement is crucial to the robustness of the results. To summarize the effect of the conditioning techniques, the difference between randomly selected tips in a freshly fabricated array is significant enough to cause order-of-magnitude disparity in emission current – only a small fraction of tips emit appreciably pre-conditioning.

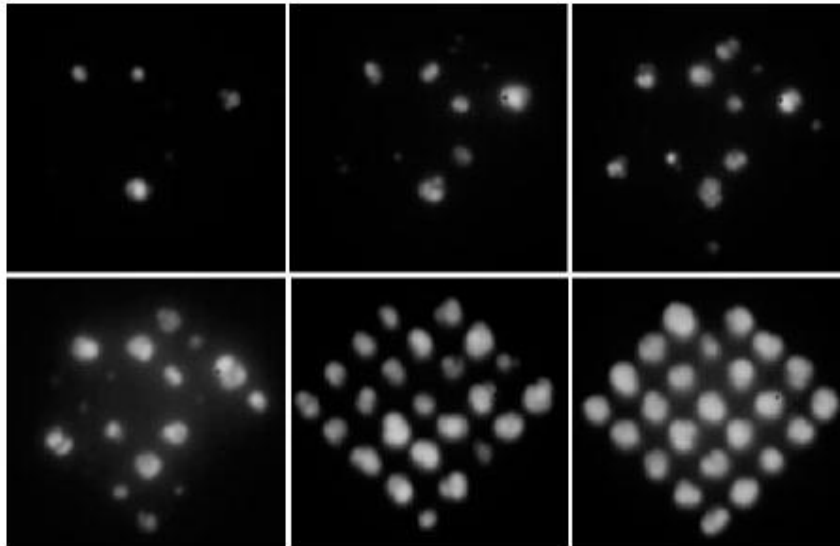


Figure 3: Progressive phosphor images of high-current conditioning of a 5x5 DFEA [8].

Fabrication error occurred on the uppermost tip during production.

Altering the tips of the array to the point at which they sufficiently resemble each other with respect to geometry and reaction to applied fields is the only way to allow results measured from a single tip to be generalized to any other tip. The conditioning is vital from a practical standpoint as well; aligning two micron-scale objects while keeping them relatively coplanar is essentially impossible with the equipment available. To achieve any reasonably high probability of successful alignment of a tip with the aperture, a shotgun approach is necessary, which necessitates the possession of an array with a high density of similarly emitting tips.

The energy analyzer is a retarding mesh design modeled after the one used in [2]; this design is used because it allows for the measurement of absolute beam energy. Figure 4 and Figure 5 show respectively the geometry and wiring of the analyzer. The electron beam enters through the front aperture and is focused by a charged cylindrical electrode such that it encounters the mesh normal to the plane of the mesh. The mesh bias is swept from through a $\sim 10\text{V}$ range from negative to positive which includes the beam energy, allowing electrons with energy less than the relative mesh bias to pass. The full sweep of the mesh bias thus produces an integrated signal, similar to the ones in Figure 7. The beam is then collected by a Faraday cup composed of a metallized phosphor screen. The phosphor screen is electrically isolated so a booster voltage can be applied to it; this

allows the analyzer to have a “viewing mode”, in which the phosphor visually shows characteristics of the beamlet. This mode is useful for checking focusing and provides qualitative information about the surface activity.

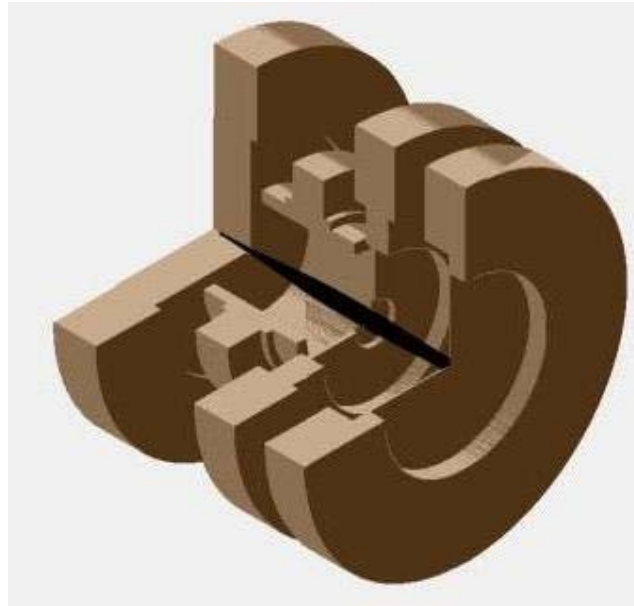


Figure 4: Cutaway view of the analyzer geometry.

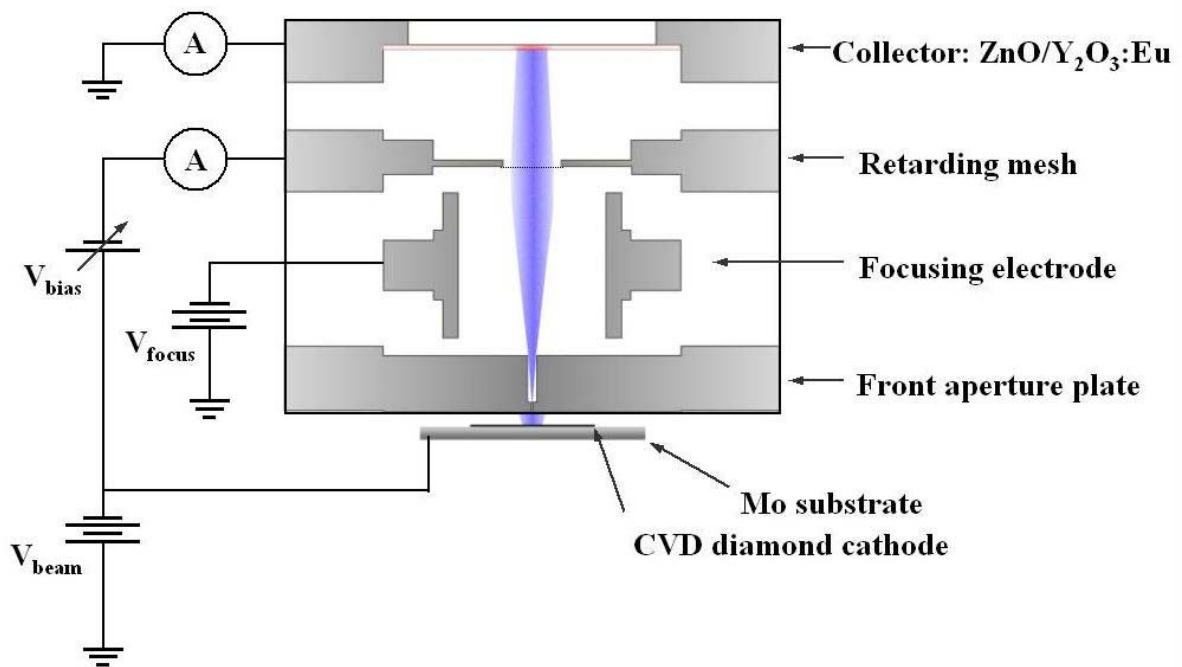


Figure 5: Wiring diagram of the analyzer with DFEA in place. Illustration by J.D. Jarvis.

The focusing optics were simulated in SIMION 7.0 to model the dependence of required focusing bias on initial beam position and angle. The chromatic aberration produced by the geometry used was negligible across beams with energy spreads much larger than those measured. A monochromatic beam with angular spread of 5 degrees (the maximum allowed by the apertures) was used to find the response to focusing (Figure 6). The optimal focusing was found to be

$$V_{focus} = V_{cathode} + |V_{cathode} - V_{anode}|$$

Using the optimum focusing, the analyzer was then simulated with a variety of energies of monochromatic beam and with large-spread beams near the predicted operating energies. The analyzer reproduced the spread of the simulated beams with millivolt-scale resolution, which is smaller than the ripple in the measurement electronics. The resolution of the analyzer was even so precise in the simulations of the monochromatic beams as to resolve the kinetic energy error in the simulation (Figure 7). The focusing bias was then tested across a narrow range including the optimum focus; several volts of deviation were required before significant widening of the measured spectrum was introduced, indicating that any ripple in biases would not affect the result of the measurement.

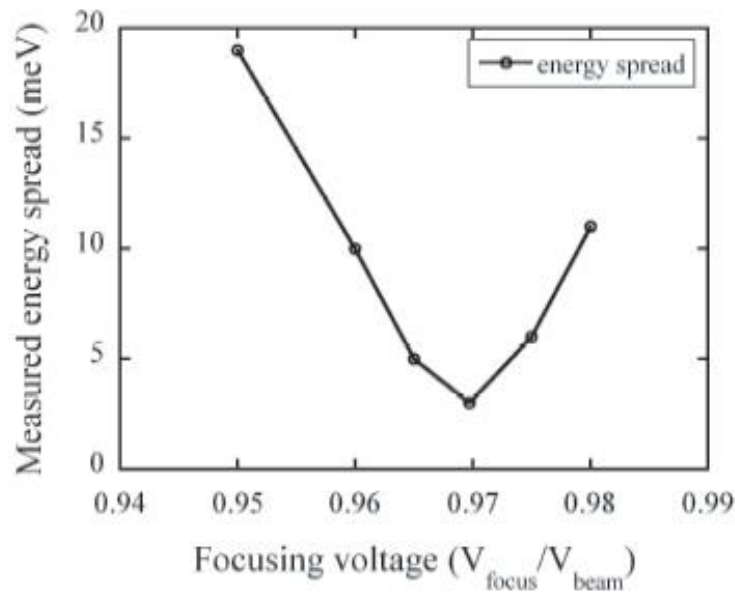


Figure 6: FWHM of simulated monochromatic beam as a function of V_{focus} .

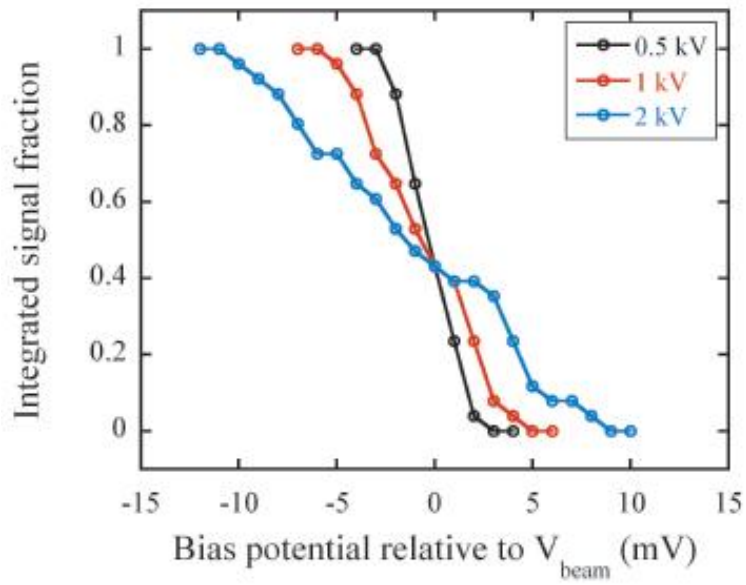


Figure 7: Integrated signal of three beam energies; optimum focusing used.

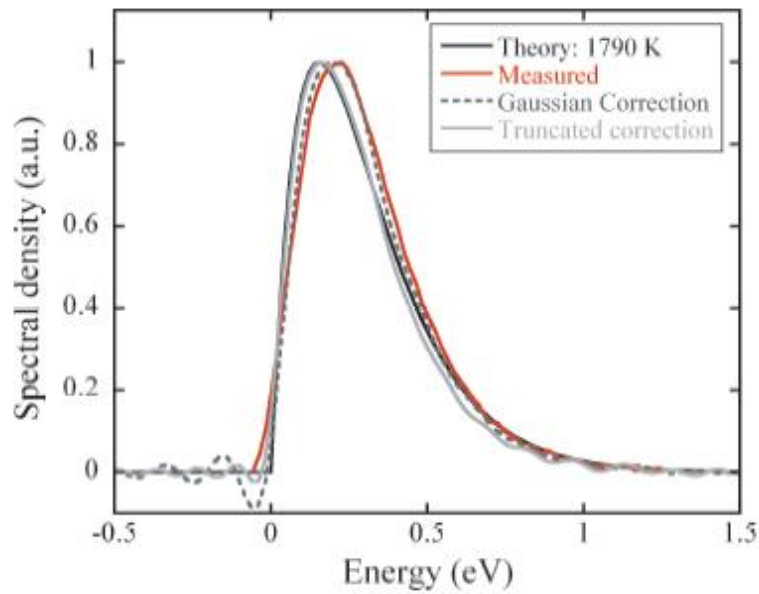


Figure 8: Theoretical, measured, and corrected thermionic spectra from experimental resolution tests.

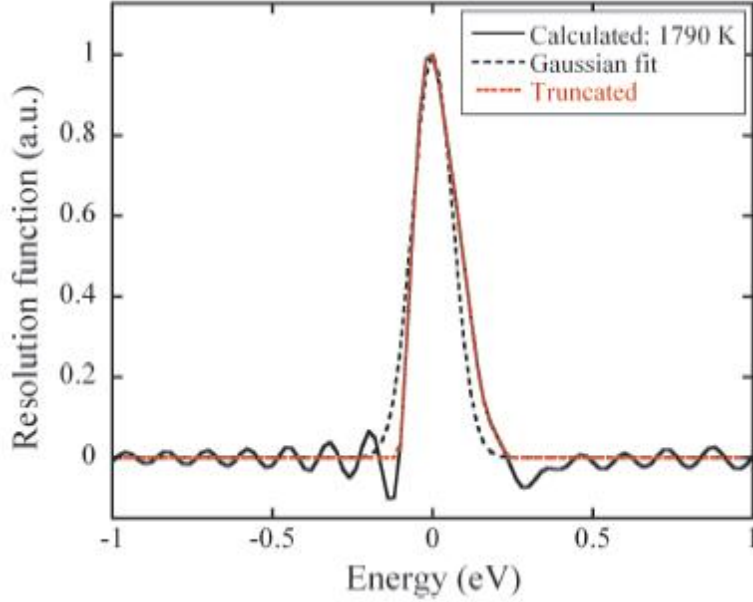


Figure 9: Calculated and Gaussian-approximated response function of the analyzer; truncation occurs at the first zero to eliminate non-physical results.

To test the resolution of the analyzer, we compared the experimentally measured distribution to the theoretically predicted spectrum for a thermionic cathode, analogous to the procedure used by Reifenberger, et al [3]. Thermionic emitters are well-known to produce current according to [7]:

$$I = AT^2 e^{-\phi/kT}$$

A LaB₆ thermionic cathode was used for the experimental tests because of the hard edge of the energy distribution of thermionic emitters at the work function as shown in Figure 8.. The low work function (~2.6eV) of LaB₆, its precise theoretical characterization and availability influenced the choice of material. The hard edge effectively sweeps out the instrumental broadening function of the analyzer and the measured distribution is a convolution of the real emission distribution with the broadening function. The instrumental broadening results from several factors, but the most noteworthy is field non-uniformity near the mesh (since it is not, as modeled, an infinitesimally thin sheet) which admits lower-energy electrons than would be admitted through normally at a given mesh bias. This results in an asymmetry in the response function. The temperature of the LaB₆ cathode during the test was approximately 1790K; the measured spectrum is normalized to the

theoretical distribution and the peaks are aligned to give a good indication of the accuracy of the device (Figure 8).

The relationship between the measured and known distributions and the resolution function is [3]:

$$j'_e(\varepsilon_m) = \int_{-\infty}^{\infty} j'_o(\varepsilon) T'(\varepsilon_m - \varepsilon) d\varepsilon$$

where j'_e is the measured spectrum, j'_o is the known spectrum, and T' is the response function. ε_m is the mesh potential relative to the Fermi energy of the cathode. Fourier transforms were then used to deconvolve and extract the analyzer response function. The function can be mapped numerically, but it is much easier to operate with when approximated with a Gaussian (Figure 9). The Gaussian approximation ignores the asymmetry of the response function (which can be seen in the incomplete correction to the peak value of the spread in Figure 8), but with a proper choice of standard deviation, it is not only very close to the numerical model, but also greatly reduces high-frequency oscillations on the function that result from the deconvolution operations. The FWHM of the analyzer response function is 0.147eV, which is smaller than the overall width (0.2 - 0.3eV) of the energy spectrum and more than small enough to detect the possible resonance effects of field emission energy spectra.

IV. Results

When operating in “viewing mode”, we can see the beam image on the phosphor; the overall view has several notable features. First, there is a hard shadow cast by the aperture as the tilt of the cathode is adjusted relative to the analyzer that obscures the beam before the tilt is large enough to sweep across another tip. This, along with the geometry of the anode/cathode spacing and the pitch of the array tells us that we are viewing a single tip. Second, the shadow of the retarding mesh is visible; the squareness of the mesh holes near the center tells us that the longitudinal axis of the beam is normal to the plane of the mesh, and the amount of distortion toward the edges of the beam spot indicate the amount of spherical aberration resulting from the focusing optics. Third, there are

multiple bright spots on the phosphor screen at any given time that fluctuate temporally on the order of seconds and are scattered across the image of the beam in a non-ordered fashion – these are the beamlets emitted from adsorbates. These adsorbates provide the bulk of the emission from the tip, as evidenced by the relative dimness of the rest of the image; the domination of the total emission by adsorbates is consistent with previous studies of adsorption effects in field emission.

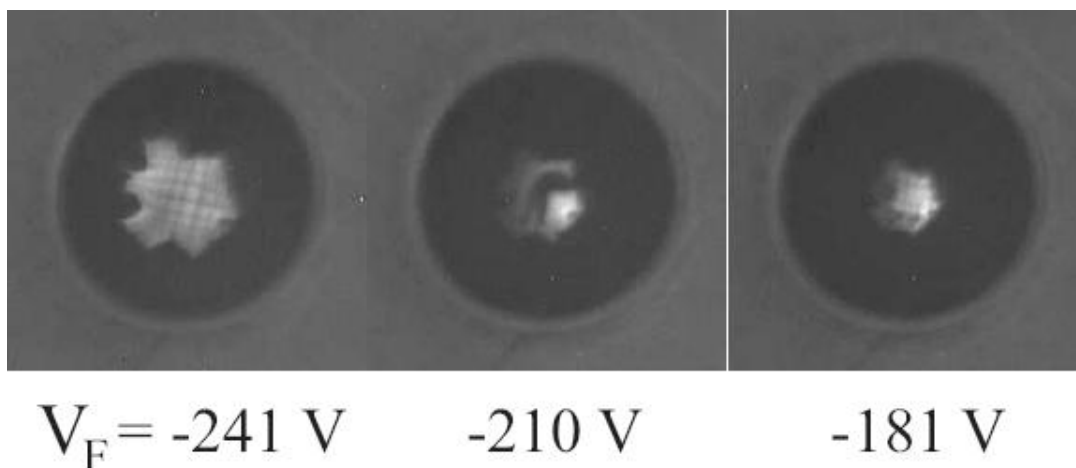


Figure 10: Phosphor images of the beam admitted into the analyzer at different focusing voltages.

Note the brighter spots and mesh shadow.

Because there are many adsorbate molecules emitting into the analyzer during any scan, the spectra vary widely. With the exception of the two averaged scans which were noted, each scan was the result of 3 to 5 sweeps of the mesh bias and was taken while the emitting surface viewed by the analyzer was in a certain state; if the emission changed, the scan was discarded and restarted. In some cases, there was a stable assortment of adsorbed molecules which would produce an energy spectrum with multiple peaks or shoulders.

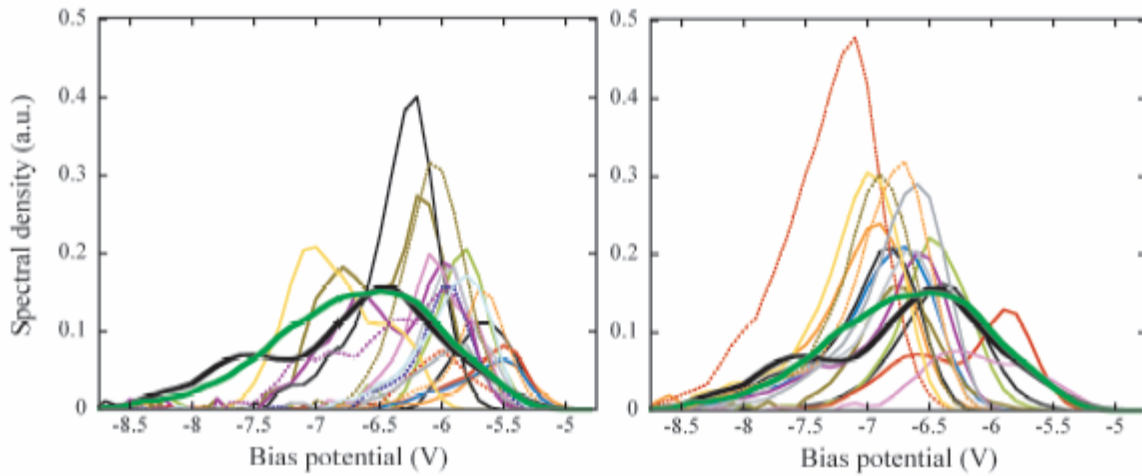


Figure 11: Assortments of spectra taken from a DFEA. The thick black and green lines are averaged over several hundred sweeps of the mesh bias.

There was a high degree of variability in the height of the spectra: the current range spans an order of magnitude. Despite this, the FWHM of single-peaked scans remained fairly invariant; most were between 0.4eV and 0.6eV, with the majority toward the low end of that range. The event (Figure 12) which produced the tallest spectrum resulted in an order-of-magnitude increase in tip current while maintaining a FWHM of ~ 0.4 eV.

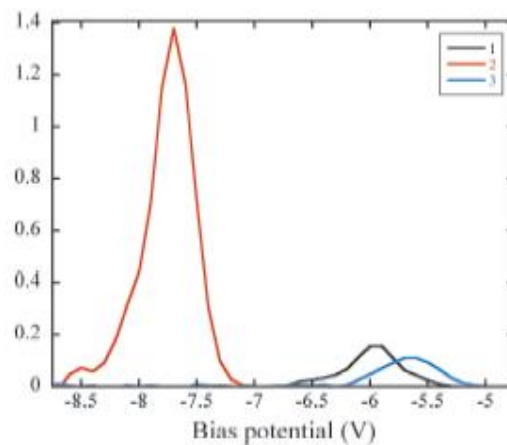


Figure 12: Event which produced a very tall spectrum with a small FWHM; other spectra are shown for comparison.

The central energy of the admitted beam ranged over several eV and appeared to be related

to the current emitted by the beamlet. The strong correlation of tall spectra with low central energies supports this. A change in central energy of the beam could also be intentionally induced by raising or lowering the accelerating field – increasing the field lowered the central energy and decreasing the field raised the central energy, both in a reproducible and seemingly linear fashion. We suspect it may be due to a potential drop along the tip, and although this has yet to be confirmed, it would be consistent with the Ohmic nature of the electron supply function in semiconductors under large currents.

Given that adsorbates seem to produce a myriad of effects, it was difficult to divine the spectrum of a clean tip from the circus of spectra in hand. Since we knew that the presence of adsorbed molecules enhanced emission and that high-current scans tended to have a low central energy, the ansatz was that the clean spectrum would be one of the ones with low current and high central energy. There were a number of these, most of which were similar in both aspects – their spectra peaked at about -5.5V mesh bias relative to the applied field.

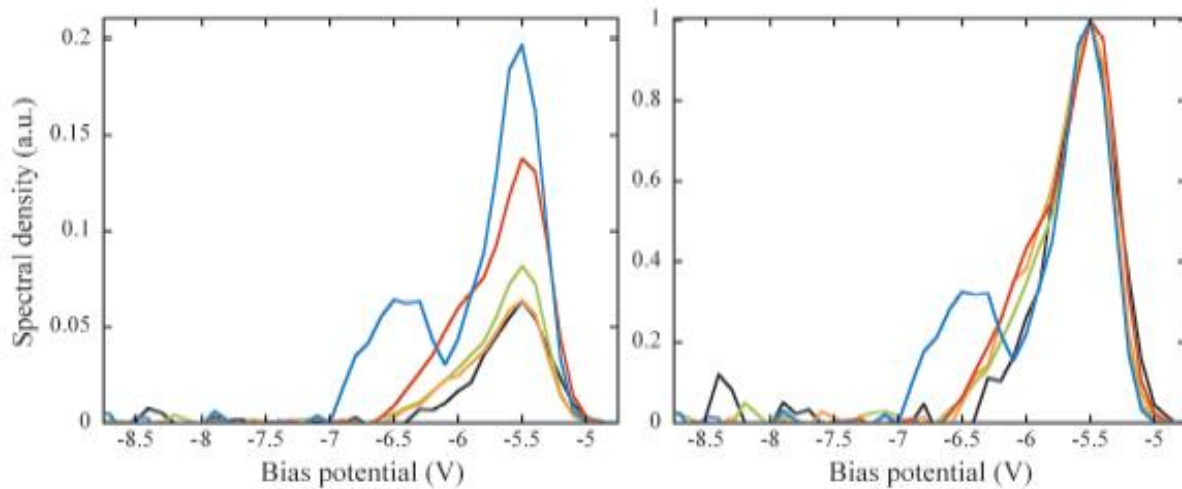


Figure 13: Left: candidates for spectra from clean diamond tip. Right: spectra are normalized with respect to peak current.

The chosen spectrum was corrected with the resolution function and fit to thermal field emission theory. Several work functions were tested; $\Phi = 5\text{eV}$ was the closest fit to the peak value. Since the exact temperature and surface field were not known, they were the chosen as the free

parameters for the fit. The best fit was found at $T = 767^\circ\text{C}$ and $F = 3.88 \times 10^3 \text{ MV/m}$. The fit is suspect due to the unexpectedly high value of T ; though, as noted, Joule-heating of the cathode does occur, the per-tip current was about 30 nA , which seems too low to produce such substantial heating. On the other hand, this is still well below the graphitization temperature which would dramatically alter the tip surface, so despite being very high, it is not impossible. The width of the spectrum is similar to those reported from a nitrogen-doped diamond-like carbon film [4]

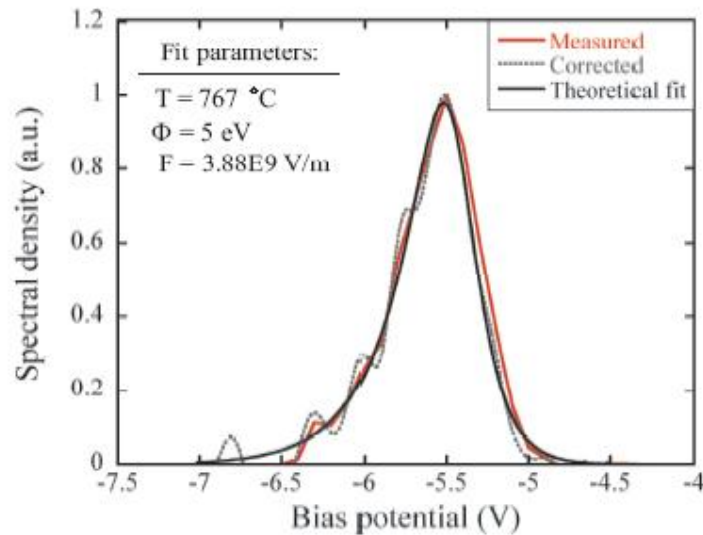


Figure 14: The spectrum of the clean diamond candidate as-measured and with instrumental resolution correction. A thermal field-emission model was used for fitting.

V. Conclusion

Fowler-Nordheim predictions seem to work reasonably well for the DFEA, but the domination of the emission by adsorbates begs further study; the dependence of these transient gas particles on both the vacuum environment and the operating temperature hints at the possibility of using the DFEA with varying amounts and types of purposeful surface contamination. The energy spread in both the clean and in many of the dirty surface states is more than small enough for many applications.

There are several further measurements which would be of great benefit. First and foremost,

the measurement of what is a conclusively clean tip would both extend the applicability of these results to devices in which adsorbates are non-factors, such as superconducting electron guns, and also provide a good lens through which to view the adsorbate-driven emission data. A heating element is being integrated into the cathode holder so adsorbates may be driven off quickly without operating at high current. Second, modifying the geometry of the experiment to allow for multi-tip measurements would qualify the extent of the generalizability of single-tip data. Third, the analyzer can be used to measure emission from a CNT; apparatus with this purpose in mind has been constructed, and preparations are being made to study the intentional placement of adsorbate atoms on the tip of a CNT. The energy analyzer and the understanding of its properties developed for its original purpose will prove to be great tools in the pursuit of all these endeavors.

References

- [1] W. P. Dyke and W. W. Dolan. Field emission. *Advances in Electronics and Electron Physics*, **Vol. 8**. Academic Press, Inc: New York, 1956.
- [2] Y. Cui, Y. Zou, A. Valfells, M. Reiser, M. Walter, I. Haber, R. A. Kishek, S. Bernal, and P. G. O'Shea. Design and operation of a retarding field energy analyzer with variable focusing for space-charge-dominated electron beams . *Review of Scientific Instruments*, **75**(2736), 2004.
- [3] R. Reifenberger, H. A. Goldberg, and M. J. G. Lee. Measurement of the total energy distribution in photo-induced field emission. *Surface Science*, **83**(599), 1979.
- [4] O. Groning, O. M. Kottel, P. Groning, and L. Schlapbach. Field emitted electron energy distribution from nitrogen-containing diamondlike carbon. *Applied Physics Letters*, **71**(16), 1997.
- [5] J. W. Gadzuk. Single-atom point source for electrons: Field-emission resonance tunneling in scanning tunneling microscopy. *Physical Review B*, **47**(19), 1992.
- [6] H. Kiesel, A. Renz, and F. Hasselbach. Observation of Hanbury Brown-Twiss anticorrelations for free electrons. *Nature*, **418**(392), 2002.
- [7] C. H. Boulware, J. D. Jarvis, H. L. Andrews, and C. A. Brau. Needle cathodes for high-brightness beams. *Vanderbilt University, Nashville, TN 37235 USA*.
- [8] J.D. Jarvis. Development of high-brightness electron sources for free-electron lasers. Doctoral dissertation. *Vanderbilt University, Nashville, TN 37235 USA*. 2009.